Viewing Early Stages of Guanine Nucleotide Attack on Pt(II) Complexes Designed with In-Plane Bulk to Trap Initial Adducts. Relevance to *cis*-Type Pt(II) Anticancer Drugs

Susan Onuschak Ano,[†] Francesco P. Intini,[‡] Giovanni Natile,*[,‡] and Luigi G. Marzilli*[,†]

Department of Chemistry, Emory University Atlanta, Georgia 30322
Dipartimento Farmaco-Chimico, Facoltà di Farmacia Università degli Studi di Bari, 70125 Bari, Italy

Received April 21, 1997

The major adduct of the anticancer drug *cis*-$PtCl_2(NH_3)_2$ with DNA, the molecular target, is an intrastrand cross-link between N7's of adjacent HH guanine (**G**) residues (HH = head-to-head, Figure 1).[1−4] However, the head-to-tail (HT) forms (Figure 1), characteristic of the minor interstrand adducts,[5−7] are thermodynamically favored in all simple *cis*-$PtA_2\mathbf{G}_2$ models (A = an amine or one-half of a diamine; **G** = guanine derivative), and the HH form is rare.[8,9] Solution data on *cis*-$PtA_2\mathbf{G}_2$ always refer to systems at equilibrium. However, because Pt substitution chemistry is kinetically controlled, it is important to understand fundamental chemistry relevant to the kinetic pathway. We present a new PtA_2 system exhibiting the normal equilibrium HT preference but designed to trap the initial products of the second Pt−N7 bond formation; the remarkably long-lived adducts allow facile characterization. This trapping has led to the quite unexpected observation that the HH atropisomer is the kinetically favored form.

Our unprecedented new findings were obtained with **Bip**Pt complexes (A_2 = 2,2′-bipiperidine, Figure 2), a system designed to concentrate the A_2 bulk near the PtN_4 coordination plane, thereby decreasing the dynamic nature of the adducts. Normally the **G** base planes are nearly perpendicular to the PtN_4 plane,[10] and the bases are free to wag and rotate through the plane; the fluxionality of the typical adduct, even for oligonucleotides, has confounded the analysis of solution properties.

When the *cis*-PtA_2 moiety is C_2 symmetrical, three *cis*-$PtA_2\mathbf{G}_2$ atropisomers (Figure 1) give four H8 ^{1}H NMR signals, two for the HH and one each for the two HT atropisomers. However, only a single H8 signal is observed in typically fluxional adducts.[11−13] Bulky A_2 ligands slow the **G** rotation rate to the NMR time scale,[9,11,13−18] and only two H8 signals were usually observed; these were attributed to a mixture of the two HT conformers.[13] The first evidence for an HH rotamer in solution came much later[9] with the observation of two additional, well-dispersed, weak H8 signals of equal intensity. This dispersion is a hallmark of HH species.[19,20]

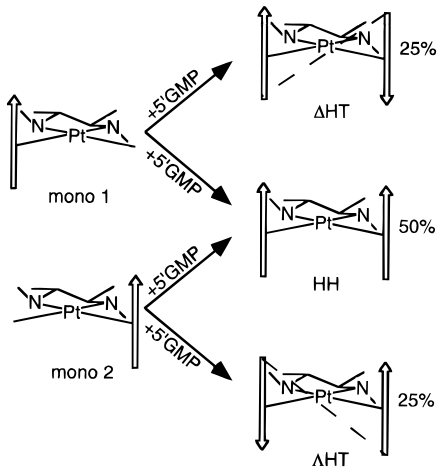

Figure 1. (Right) **G** orientations in the three (*S,R,R,S*)-**Bip**Pt(5′GMP)$_2$ atropisomers. In the scheme, the 5′GMP coordination sites are forward and the **Bip** ligand is to the rear and mostly omitted for clarity. The arrows represent the **G** bases with the H8 at the head. The dotted lines joining the tails define the HT chirality. A hypothetical scheme shows how the statistical distribution could arise from the two possible mono species (left).

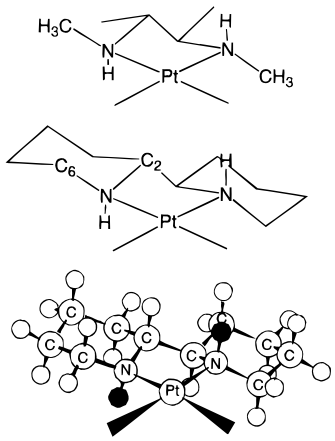

Figure 2. View of moieties with (*S,R,R,S*) ligands. Ball and stick (bottom) and sketch (middle) of **Bip**Pt and sketch (top) of **Me$_2$DAB**Pt.

We employed **Bip**Pt$(NO_3)_2$ with (*S,R,R,S*) or (*R,S,S,R*) asymmetric centers at the N, C, C, and N chelate ring atoms. Since results at pH 3 and 7 were very similar, we describe the studies at pH 3, because the 5′GMP has the same 1$^-$ charge as **G** in polymers and **Bip** NH exchange to ND is slow, allowing the use of the NH signals. On treatment of (*S,R,R,S*)-**Bip**Pt$(NO_3)_2$ with ∼3 equiv of 5′GMP in D_2O, *the initial ^{1}H NMR spectrum (14 min) contained four H8 signals nearly equal in intensity, indicating that fully 50% of the (S,R,R,S)-**Bip**Pt(5′GMP)$_2$ formed must be the HH atropisomer, seen previously as only a very minor species (Figure 3)*; the free 5′GMP H8

[†] Emory University.
[‡] Università degli Studi di Bari.

(1) Fichtinger-Schepman, A. M. J.; Lohman, P. H. M.; Reedijk, J. *Biochemistry* **1985**, *24*, 707−713.
(2) Eastman, A. *Biochemistry* **1986**, *25*, 3912−3915.
(3) Fichtinger-Schepman, A. M. J.; van Oosterom, A. T.; Lohman, P. H. M.; Berends, F. *Cancer Res.* **1987**, *47*, 3000−3004.
(4) Takahara, P. M.; Rosenzweig, A. C.; Frederick, C. A.; Lippard, S. J. *Nature* **1995**, *377*, 649−652.
(5) Sip, M.; Schwartz, A.; Vovelle, F.; Ptak, M.; Leng, M. *Biochemistry* **1992**, *31*, 2508−2513.
(6) Huang, H.; Zhu, L.; Reid, B. R.; Drobney, G. F.; Hopkins, P. B. *Science* **1995**, *270*, 1842−1845.
(7) Paquet, F.; Pérez, C.; Leng, M.; Lancelot, G.; Malinge, J.-M. *J. Biomol. Struct. Dyn.* **1996**, *14*, 67−77.
(8) Lippert, B.; Raudaschl, G.; Lock, C. J. L.; Pilon, P. *Inorg. Chim. Acta* **1984**, *93*, 43−50.
(9) Xu, Y.; Natile, G.; Intini, F. P.; Marzilli, L. G. *J. Am. Chem. Soc.* **1990**, *112*, 8177−8179.
(10) Iwamoto, M.; Mukundan, S., Jr.; Marzilli, L. G. *J. Am. Chem. Soc.* **1994**, *116*, 6238−6244.
(11) Marcelis, A. T. M.; Korte, H.-J.; Krebs, B.; Reedijk, J. *Inorg. Chem.* **1982**, *21*, 4059−4063.
(12) Cramer, R. E.; Dahlstrom, P. L. *Inorg. Chem.* **1985**, *24*, 3420−3424.
(13) Cramer, R. E.; Dahlstrom, P. L. *J. Am. Chem. Soc.* **1979**, *101*, 3679−3681.
(14) Marcelis, A. T. M.; van der Veer, J. L.; Zwetsloot, J. C. M.; Reedijk, J. *Inorg. Chim. Acta* **1983**, *78*, 195−203.
(15) Dijt, F. J.; Canters, G. W.; den Hartog, J. H. J.; Marcelis, A. T. M.; Reedijk, J. *J. Am. Chem. Soc.* **1984**, *106*, 3644−3647.
(16) Miller, S. K.; Marzilli, L. G. *Inorg. Chem.* **1985**, *24*, 2421−2425.
(17) Cramer, R. E.; Dahlstrom, P. L.; Seu, M. J. T.; Norton, T.; Kashiwagi, M. *Inorg. Chem.* **1980**, *19*, 148−154.
(18) Kiser, D.; Intini, F. P.; Xu, Y.; Natile, G.; Marzilli, L. G. *Inorg. Chem.* **1994**, *33*, 4149−4158.
(19) Marzilli, L. G.; Iwamoto, M.; Alessio, E.; Hansen, L.; Calligaris, M. *J. Am. Chem. Soc.* **1994**, *116*, 815−816.
(20) Alessio, E.; Hansen, L.; Iwamoto, M.; Marzilli, L. G. *J. Am. Chem. Soc.* **1996**, *118*, 7593−7600.

S0002-7863(97)01250-X CCC: $14.00

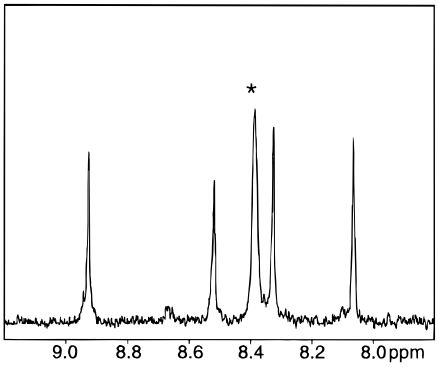

Figure 3. H8 ^{1}H NMR signals of the (*S*,*R*,*R*,*S*)-**Bip**Pt$(NO_3)_2$ + 5′GMP reaction at 14 min, 20 °C, pH ∼3. (An asterisk indicates the H8 signal of excess 5′GMP.)

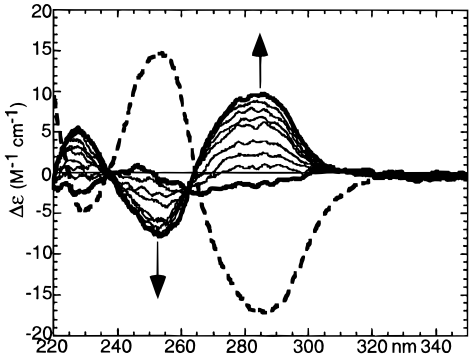

Figure 4. CD spectra of (*S*,*R*,*R*,*S*)-**Bip**Pt$(5'GMP)_2$ recorded from 20 to 280 min (arrows denote direction of peak growth) and (- - -) CD spectrum of (*R*,*S*,*S*,*R*)-**Bip**Pt$(5'GMP)_2$ at equilibrium.

signal intensity did not change with time, indicating complete reaction at 14 min. The two HH H8 signals are easily identified (equal intensity, well-separated (∼1 ppm) upfield and downfield H8 signals[9] connected by an NOE cross-peak, Supporting Information).

Since each **G** base has two possible orientations with respect to the coordination plane, a purely statistical distribution of HH: ΔHT:ΛHT atropisomers is thus 2:1:1 (Figure 1), more or less the result observed for (*S*,*R*,*R*,*S*)-**Bip**Pt$(5'GMP)_2$. The results for (*R*,*S*,*S*,*R*)-**Bip**Pt$(5'GMP)_2$ were almost statistical, 4:3:3. Thus, this bulky A_2 ligand has little influence on the orientation of the second attacking base as it adds to Pt. The relatively sterically undemanding A_2 ligands in the better anticancer agents are extremely unlikely to influence **G** attack orientation. Such agents most probably form considerable HH adduct, which is undoubtedly too short-lived to be observed. No HH species above the equilibrium amount can be detected even for **Me$_2$DAB**Pt$(5'GMP)_2$ (**Me$_2$DAB** = *N*,*N*′-dimethyl-2,3-diaminobutane, Figure 2), one of the few cases where HH species can be discerned.[9] The main difference between **Bip** and **Me$_2$DAB** is that **Me$_2$DAB** is acyclic; the relative rigidity of the **Bip** rings has dramatic effects on dynamics but little influence on structure or energetics. No magnetization transfer resulting from interconversion between any (*R*,*S*,*S*,*R*)-**Bip**Pt-$(5'GMP)_2$ or (*S*,*R*,*R*,*S*)-**Bip**Pt$(5'GMP)_2$ rotamers was seen in 1D saturation transfer experiments *even at 80 °C*. In contrast, whereas no H8 EXSY cross-peaks were observed in any **Bip**Pt NOESY spectra (see below), strong EXSY cross-peaks were observed, even at 5 °C, for **Me$_2$DAB**Pt$(5'GMP)_2$.[9] However, the shifts of all four H8 signals and the equilibrium distribution are nearly identical for the **Bip** and **Me$_2$DAB** complexes; this similarity to a more typical dynamic complex adds validity to our in-plane bulk design and supports our suggestion that the initial predominant *cis*-PtA_2**G**$_2$ adduct is HH for most (if not all) cases.

Since redistribution of the atropisomers of (*S*,*R*,*R*,*S*)-**Bip**Pt-$(5'GMP)_2$ and (*R*,*S*,*S*,*R*)-**Bip**Pt$(5'GMP)_2$ was so slow, we hypothesized that the process could be monitored for the first time in *cis*-PtA_2**G**$_2$ systems by CD spectroscopy. The **Bip**Pt-$(NO_3)_2$ isomers were treated with 4 equiv of 5′GMP and allowed to react for 10 min at high NMR concentrations before the solutions were diluted to 20 μM for CD spectral acquisition (10 min). For (*S*,*R*,*R*,*S*)-**Bip**Pt$(5'GMP)_2$, there were initially no distinct CD maxima (Figure 4). Thus initially when the HH rotamer is dominant, no distinct CD feature is associated with it. Over 280 min, positive (284 nm) and negative (254 nm) peaks grew (Figure 4). Similar behavior was observed for (*R*,*S*,*S*,*R*)-**Bip**Pt$(5'GMP)_2$, except that the signs of the CD peaks were reversed. Thus, the **Bip** ligand is stereochemically controlling, with the different orientation of the N substituents determining the HT chirality (since **G** itself has chiral centers, an exact enantiomeric set of atropisomers is not possible).

2D NOESY and double quantum filtered (DQF) COSY experiments at 5 °C for *rac*-**Bip**Pt$(5'GMP)_2$ were used to assign signals for all atropisomers simultaneously. For the major HT atropisomer of (*R*,*S*,*S*,*R*)-**Bip**Pt$(5'GMP)_2$ and of (*S*,*R*,*R*,*S*)-**Bip**Pt$(5'GMP)_2$ at equilibrium, strong H8−NH and H8−C6H$_{eq}$ NOE cross-peaks were found, and H8−H6H$_{ax}$ cross-peaks were not detected. These data demonstrate that the major HT atropisomers have opposite chiralities, consistent with the CD results.

The superior characteristics of the **Bip** ligand allow us, in effect, to trap the initial forms of the adducts. These results reveal another favorable feature of the *cis*-Pt drugs contributing to activity. Apparently, in the substitution chemistry, enthalpy barriers for HT and HH adduct formation are comparable but the HH adduct formation is entropically favored. The DNA sugar−phosphate backbone also favors the HH conformation. We conclude that both the fundamental Pt substitution chemistry and the DNA chemistry contribute to the high kinetic preference for HH intrastrand over HT interstrand cross-links.

Acknowledgment. This work was supported by NIH grant GM 29222 (to L.G.M.), NATO CRG. 950376 (to L.G.M. and G.N.), and MURST (Contribution 40%), CNR, and EC (COST Chemistry project D1/02/92 (to G.N.). NSF Grant ASC-9527186 supported our use of the Internet for remote collaborative research.

Supporting Information Available: Partial 1D, 5 °C DQF COSY, and NOESY spectra of *rac*-**Bip**Pt$(5'GMP)_2$ (3 pages). See any current masthead page for ordering and Internet access instructions.

JA971250R